Materials Research Proceedings 41 (2024) 540-548 https://doi.org/10.21741/9781644903131-60

Investigation of the friction behavior of uni- and bidirectional non-crimp fabrics

SCHÄFER Bastian[1,a*], NAOUAR Naim[2] and KÄRGER Luise[1,b*]

[1]Karlsruhe Institute of Technology (KIT), Institute of Vehicle System Technology (FAST), Lightweight Engineering, Karlsruhe, Germany

[2]Université de Lyon, LaMCoS CNRS, Lyon, F-69621, France

[a]bastian.schaefer@kit.edu, [b]luise.kaerger@kit.edu

Keywords: Fabrics/Textiles, Experimental Characterization, Friction, UD-NCF, Biax-NCF

Abstract. The friction behavior of engineering textiles directly affects the forming quality during composite molding processes. In forming tests of dry engineering textiles large relative slip between plies and the tools is observed. The resulting tangential contact stresses influence the material's membrane stresses, which in turn impact the fabric's deformation and potentially lead to forming defects such as gapping or ruptures of the textile. The characterization of friction is commonly conducted via relative motion between a fabric ply and either another fabric ply (ply-ply) or a tool (tool-ply) under controlled transverse pressure. The resulting behavior of a textile reinforcement depends on the mesoscopic structure of its unit cell and the material of its constituents. In this work, the tangential friction behavior at interfaces between ply and tooling and between plies of a unidirectional and a bidirectional non-crimp fabric are investigated in sled pull-over-tests. The behavior is analyzed with respect to the applied normal forces, the relative velocity and the relative fiber orientation. A generally rate-independent behavior is observed. Tool-ply friction is only slightly affected by the applied pressure, while ply-ply friction is strongly influenced by the stitching pattern at the contact interface.

Introduction

The final fiber orientation in components manufactured from liquid composite molding processes is significantly influenced by relative slip between individual fabric layers as well as the tools. The relative movement results in tangential friction, which induces in-plane stresses and impacts the fabric's deformation. This influences the material draw-in [1] and can potentially result in defects such as gapping or ruptures of the textile [2]. Non-crimp fabrics (NCFs) have straight fibers compared to woven fabrics with undulated fibers and therefore provide a higher lightweight potential. However, they are more susceptible to defects due to the low stiffness and strength of the stitching.

The characterization of friction is commonly conducted via relative motion between a fabric ply and either another fabric ply (ply-ply) or a tool (tool-ply) under controlled transverse pressure. Usually, Coulomb's friction is assumed for the analysis of dry textiles

$$f_\mathrm{f} = \mu N, \tag{1}$$

where f_f is the tangential friction force, N is the applied normal load and μ is the coefficient of friction (CoF).

In a benchmark study, Sachs et al. [3] compared different experimental setups from three design categories for the same material, i.e. pull-out-tests, pull-through-tests and sled pull-over-tests. Comparable results were achieved for all setups, but systematic errors were observed and attributed to edge effects and uneven pressure distributions. Thus, sled pull-over- or pull-through-

tests with a sufficiently large contact area and chamfered edges were recommended. However, the sled-test was originally developed for thin plastic film materials (ASTM standard D1894-14 [4]) and therefore mainly suitable for lower transverse pressure to prevent balancing problems and stick-slip effects [2,5].

The friction behavior of a textile reinforcement depends on the mesoscopic structure of its unit cell and the material of its constituents. Protruding high points of the material are especially notable during ply-ply contact due to stick-slip or shock effects. These result from undulations in woven fabrics [6,7,8] or the stitching in non-crimp fabrics [2,9]. Additionally, pressure- and rate-dependency as well as an impact of a layer's relative orientation and deformation state (shear) are reported for dry textiles.

Tool-ply friction for dry textiles is usually found to be nearly independent of the relative velocity [3,10], of the ply's relative orientation [9,11,12] and for woven fabrics independent of shear deformation applied to the textile before testing [13]. An increasing normal pressure reduces the CoF [10,14,15,16], because of its effect on the surface roughness and true contact area between fibrous material as demonstrated by Avgoulas et al. [16] based on Hertzian theory. However, this correlation applies mainly for high pressures (> 10 kPa), while for low pressures often no or even a slightly positive influence is measured [3,16,17].

Ply-ply friction for dry textiles is also reported as nearly independent of the relative velocity [10,18], but for woven fabric increasing under shear deformation applied to the textile before testing [13]. The effective CoF between plies decreases for high transverse pressure [10,14,18], due to the lateral spreading of the fabric under compaction that results in smaller undulations and thus less shock effects [18]. The reported influence of the relative orientation is most heavily dependent on the specific material being tested. The most common observation for woven fabrics is a lower CoF for relative orientations unequal to 0° or 90° [10,19], with the lowest value often, but not always measured for 45° [6,13]. In contrast, the behavior of NCFs does not follow a distinct trend and depends on the precise architecture [2,9,12]. However, Quenzel et al. [9] recently measured an increasing CoF by decreasing the stitching length of Biax-NCFs manufactured from the same materials as it increases the number of stitch yarn loops.

In this work, the tangential friction behavior at interfaces between ply and tooling (TP) and between plies (PP) of a unidirectional (UD) and a bidirectional (Biax) NCF is investigated in sled pull-over-tests to identify the most relevant factors that influence the friction behavior. The behavior is analyzed with respect to the applied normal forces, relative velocity and relative fiber orientation as well as fabric side at the interfaces. Both NCFs are stitched in a tricot pattern, resulting in an additional influence of the fabric side that has not been investigated in previous studies on NCFs because they applied bidirectional fabrics with similar chain stitching patterns on both sides [2,9,12].

Experimental test setup and procedure

Materials. In this work, a unidirectional (UD300) and a bidirectional (MD600) non-crimp fabric, both without binder, are used. The fabrics are manufactured by Zoltek and produced from the same PX35-50K continuous carbon fiber (CF) heavy tows. Both fabrics are stitched together with a 76 dtex PES yarn in a tricot pattern. The UD-NCF consists of a single layer of aligned CF rovings with thin glass fibers (GF) on the back for improved handleability and the Biax-NCF of two layers in a 0°/90° orientation. Both fabrics have a similar number of CFs with about 300 g/m^2 in their respective main reinforcing directions.

Sled pull-over tests. The inter-ply behavior is investigated with a sled pull-over setup based on ASTM standard D1894-14 [4] mounted to a universal testing machine, cf. Figure 1. All edges on the sled are chamfered and relatively light weights are used to minimize stick-slip effects and comply with the findings of the benchmark of Sachs et al. for dry textiles [3]. The surface

roughness R_a of the sled is, similar to the roughness of a mold applied during resin transfer molding or wet compression molding, about 0.617 µm [11].

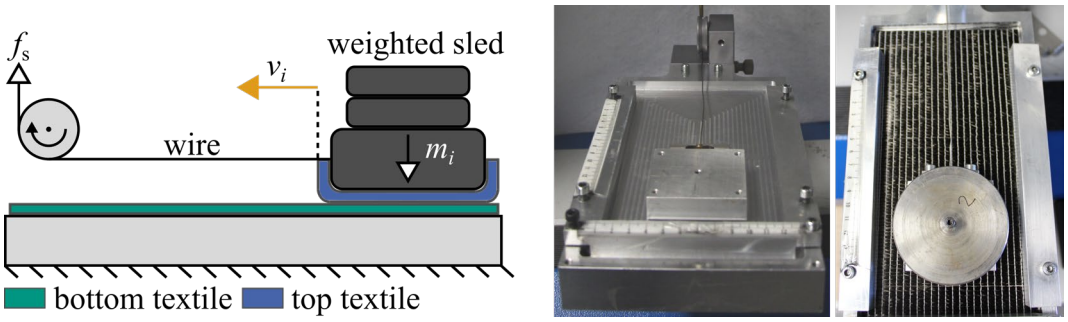

Fig. 1. Schematic illustration of the experimental friction setup and test bench on tensile machine.

A dry specimen is clamped to the bottom surface of the setup and a sled with a surface area of $65\ x\ 65\ \mathrm{mm}^2$ is pulled over a distance of 100 mm at a constant velocity v_i over the fabric to investigate tool-ply friction (TP). The influence of the applied normal force is investigated with three different sled weights of $m_i \in [218\ \mathrm{g}, 720\ \mathrm{g}, 1222\ \mathrm{g}]$. Two different velocities are applied during the tests with $v_1 = 50\ \mathrm{mm/min}$ and $v_2 = 150\ \mathrm{mm/min}$. An additional specimen is wrapped around the sled to investigate ply-ply friction (PP). The clamps used to secure the specimen to the sled and the fabric itself add weight, which is measured before each repetition and is approximately ~30-35g. The front and back of both fabrics are investigated separately due to the different visible stitching patterns. Each test is repeated at least three times for each configuration with new specimens. The fiber orientation of the visible side of each fabric is used for a consistent naming convention to investigate different fabric orientations, cf. Figure 2.

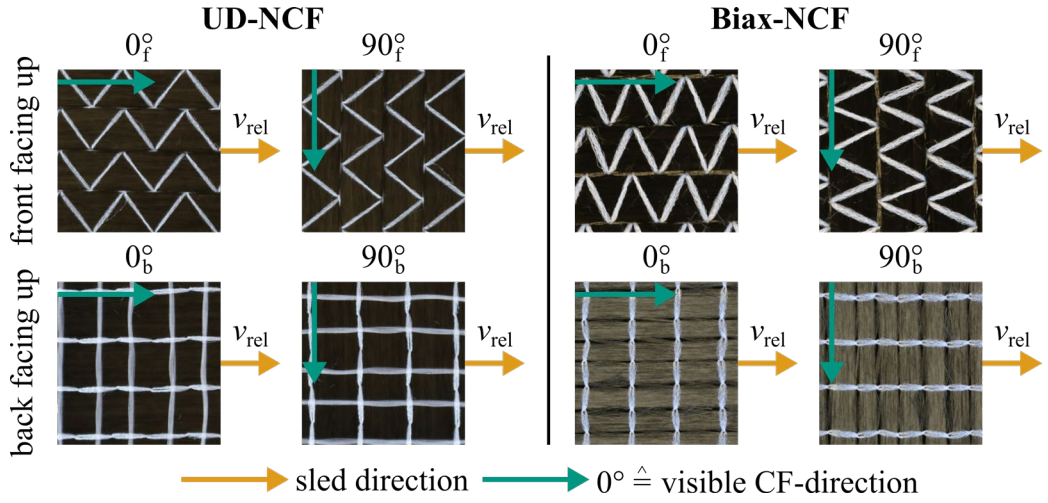

Fig. 2. Naming convention for the inter-ply characterization tests.

The measured pulling force of the sled f_s is used to calculate the resulting coefficient of friction (CoF) according to Equation 1 with:

$$\mu = \frac{f_s}{g\ m_i}. \tag{2}$$

The static CoF μ_s is obtained as the maximum value, which occurs in all tests within the first 10 mm of sled displacement due to a slight initial slag in the wire. The dynamic CoF μ_d is calculated as the average between a displacement of 40 mm and 90 mm where a steady state behavior was observed for all tests. The calculation of both CoF is demonstrated in Figure 3. The wavelength of the oscillations in the PP-tests agrees closely with the stitching pitch (7.2 mm) of UD-NCF. This behavior is similar to stick-slip and shock effects observed for other NCFs with chain stitching patterns [2,9] as well as the effect of undulations in woven fabrics [6,7,8]. The averages and standard deviations for the dynamic CoF are calculated based on the raw CoF-displacement curves of all individual tests in the desired range, rather than the standard deviation of the average CoF for each individual, to account for the magnitude of the oscillations during PP-friction. The static CoF is 5 - 20 % higher for TP-friction and 20 – 40 % for PP-friction than the dynamic CoF in all tests. However, the static and dynamic CoF show very similar tendencies in comparisons for different configurations. The results are therefore discussed below on the basis of the dynamic CoF.

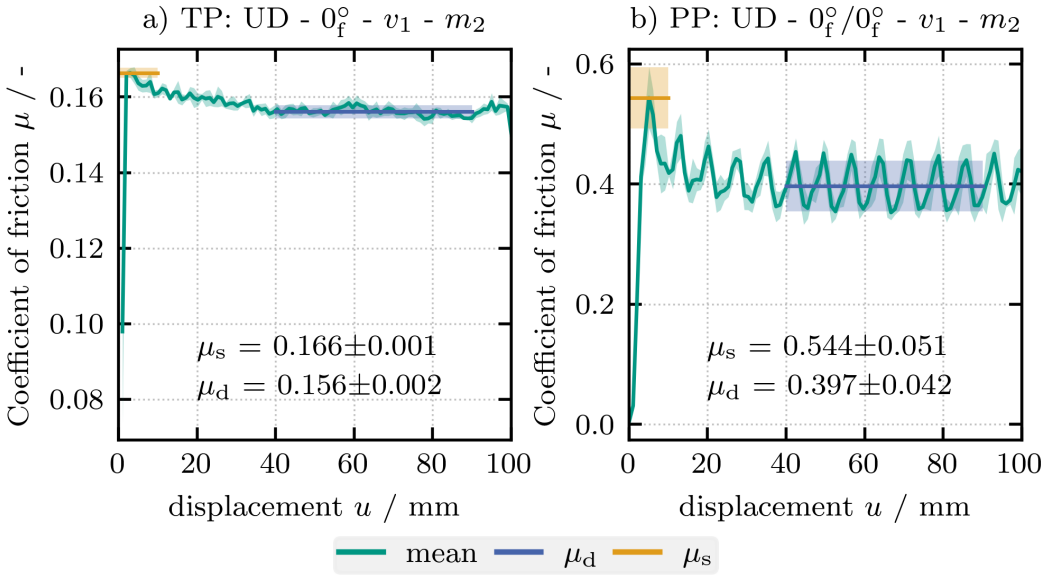

Fig. 3. Schematic illustration of the calculation of the static $\boldsymbol{\mu_s}$ and dynamic $\boldsymbol{\mu_d}$ coefficient of friction. The ±values give the standard deviation of all tests in the desired range and for the dynamic CoF represent the magnitude of the observed oscillations.

Results

Tool-ply. The influence of the sled weight and velocity on the tool-ply behavior are investigated for the 0°_f-configuration of both materials, cf. Figure 4 a. The dynamic CoF is independent of the sled velocity for both materials (same colored bars). A higher sled weight results in a slight increase of the measured μ_d (each column) for UD-NCF and reduces the standard deviation. This behavior is similar to observations for other engineering textiles at low pressure [3,16,17]. For Biax-NCF, the increase of μ_d for a higher sled weight is only significant for the higher sled velocity, but with overlapping scatter.

The influence of the fiber orientation and fabric side on the TP behavior of both materials is investigated at a constant sled weight m_2 and velocity v_1, cf. Figure 4 b. The dynamic CoF is slightly higher for the back side of UD-NCF, but no clear influence of the fiber orientation is observed. For Biax-NCF, no clear trend is observed for the ply's side or orientation.

Materials Research Proceedings 41 (2024) 540-548 https://doi.org/10.21741/9781644903131-60

Overall, Biax-NCF has a slightly higher CoF in the TP-tests despite the similar surface architecture of both fabrics. The measured dynamic CoF for both materials remains relatively small for all tests $\mu_d < 0.17$, which agrees with measurements of other dry textiles [3,9,11,13].

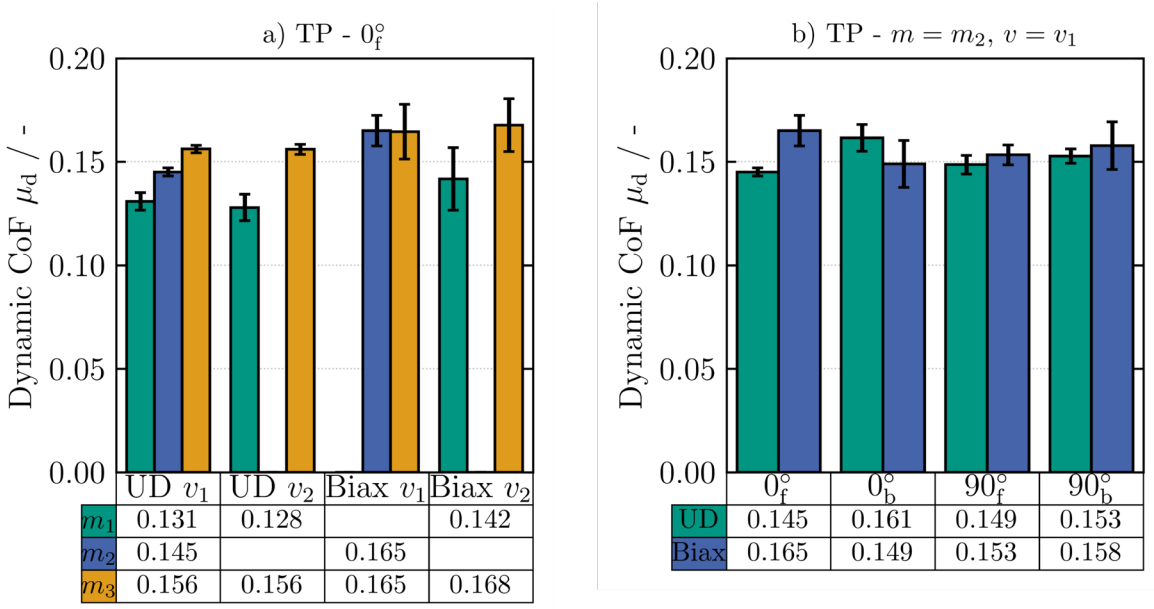

Fig. 4. Experimental results of the tool-ply (TP) dynamic CoF | (a) Influence of the applied mass $\boldsymbol{m_i}$ *and velocity* $\boldsymbol{v_i}$ *in a* $\boldsymbol{0^\circ_f}$*-configuration for both materials; (b) Influence of the relative interface orientations with an applied mass of* $\boldsymbol{m = m_2}$ *and velocity* $\boldsymbol{v = v_1}$*. The error bars indicate the standard deviation of all tests.*

Ply-Ply. The influence of the sled weight and velocity on the ply-ply behavior are investigated for the $0^\circ_f/0^\circ_f$-configuration of UD-NCF, cf. Figure 5, under the assumption of a similar behavior for the $0^\circ_f/0^\circ_f$-configuration of Biax-NCF. The dynamic CoF is independent of the sled velocity but decreases for an increasing normal pressure. The higher sled weight flattens the roving and stitching, reducing shock effects, which is reflected in the lower amplitude of the observed oscillations as indicated by the standard deviation [2,9].

Materials Research Proceedings 41 (2024) 540-548 https://doi.org/10.21741/9781644903131-60

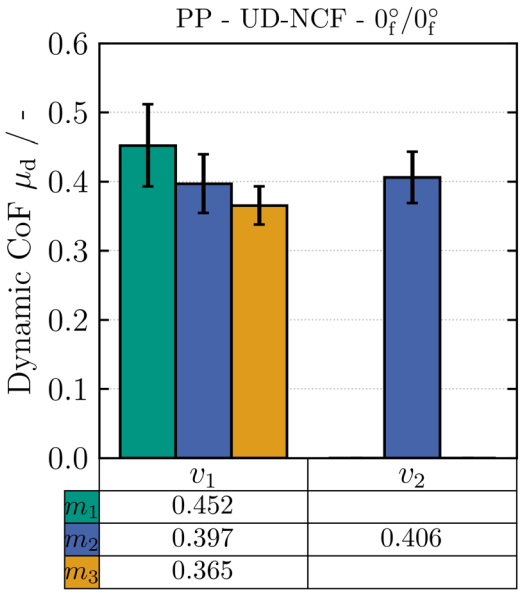

Fig. 5. Influence of the applied mass $\boldsymbol{m_i}$ and velocity $\boldsymbol{v_i}$ on the dynamic CoF for the ply-ply behavior of UD-NCF in a $\boldsymbol{0^\circ_f/0^\circ_f}$-configuration. The error bars indicate the standard deviation of all tests.

The influence of the fabric side and relative fiber orientation at the interface on the PP behavior of both materials is investigated at a constant sled weight m_2 and velocity v_1, cf. Figure 6.

First, configurations with different sides of the fabrics and the same fiber orientations at the interface are compared, i.e. $0^\circ_\square/0^\circ_\square$, $0^\circ_\square/90^\circ_\square$ and $90^\circ_\square/90^\circ_\square$. The dynamic CoF decreases for configurations with the back side of one or two plies at the interface for both fabrics (e.g. $0^\circ_f/0^\circ_f > 0^\circ_f/0^\circ_b > 0^\circ_b/0^\circ_b$). This effect is observed independent of the relative fiber orientation at the interface. The stitching on the front side of the fabric with the tricot pattern covers a larger area of the ply and thus offers more opportunities for interlocking with another ply, presumably causing the higher μ_d. A particularly high amplitude of the oscillations is measured for the $0^\circ_b/0^\circ_b$-configuration of Biax-NCF, which is presumably caused by significant shock effects due to the linear stitching pattern on the back side. This behavior is not observed for UD-NCF because the linear stitch pattern is recessed between the rovings instead of crossing rovings on the back as for Biax-NCF, cf. Fig. 2.

Second, configurations with similar sides of the fabric and different fiber orientations are compared, i.e. $\square^\circ_f/\square^\circ_f$ for both materials and additional $\square^\circ_f/\square^\circ_b$ for UD-NCF. A decrease of μ_d is measured for more 90° plies when both tricot stitch patterns on the front are in contact (e.g. $0^\circ_f/0^\circ_f > 0^\circ_f/90^\circ_f > 90^\circ_f/90^\circ_f$). This effect is notably stronger for Biax-NCF and only very small for UD-NCF. It is not observed in the $\square^\circ_f/\square^\circ_b$ -configurations of UD-NCF.

Overall, the CoF for PP-contact is significantly higher compared to the TP-contact and strongly influenced by the specific configuration of the stitching at the interface.

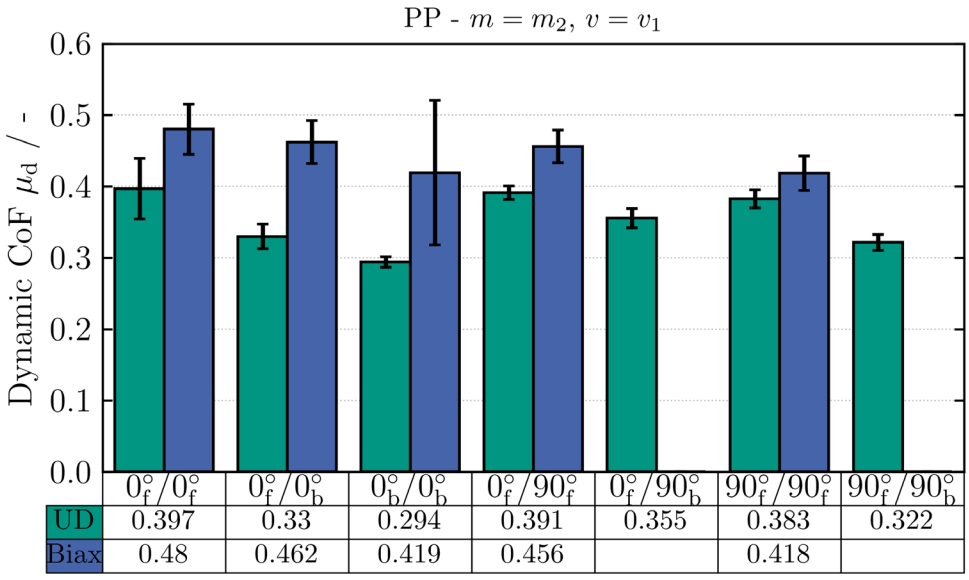

	$0^\circ_f/0^\circ_f$	$0^\circ_f/0^\circ_b$	$0^\circ_b/0^\circ_b$	$0^\circ_f/90^\circ_f$	$0^\circ_f/90^\circ_b$	$90^\circ_f/90^\circ_f$	$90^\circ_f/90^\circ_b$
UD	0.397	0.33	0.294	0.391	0.355	0.383	0.322
Biax	0.48	0.462	0.419	0.456		0.418	

Fig. 6. Influence of the relative interface orientations on the dynamic CoF for the ply-ply behavior with an applied mass of $\boldsymbol{m = m_2}$ and velocity $\boldsymbol{v = v_1}$. The error bars indicate the standard deviation of all tests.

Summary and discussion

The friction behavior of a UD- and a Biax-NCF is investigated for different configurations at the tool-ply as well as ply-ply interfaces. A comprehensive analysis is conducted based on the dynamic CoF to evaluate the influences of the applied normal forces, relative sled velocity, fabric side and relative fiber orientation at the interfaces.

The inter-ply behavior of UD- and Biax-NCFs is significantly different for ply-ply (PP) compared to tool-ply (TP) contact. The tangential friction is rate-independent for both cases and significantly higher CoF are measured during PP-contact compared to TP-contact. For an increased sled weight, the CoF increases slightly for TP-contact and notably decreases for PP-contact. This effect can be explained for PP-contact due to flattening of the rovings and stitching for increased normal pressure. The positive pressure-dependency during TP-contact is also observed for other engineering textiles at low pressure [3,16,17], but no conclusive reason is known.

The relative fiber orientation between two plies has no significant influence, except for a slight reduction of $\mu_d$for Biax-NCF, in contrast to the behavior of woven fabrics [6,10,13,19]. Instead, the most relevant factor for the PP-behavior of both materials is the architecture of the contacting side of the fabric. Configurations with plies in contact with the zigzag pattern of the tricot stitching on the front have a notably higher CoF due to the increased opportunities for interlocking. Additionally, the stitching pattern results in strong oscillations in the measured behavior due to stick-slip and shock effects, similar to the observations for undulations in woven fabrics. The measured μ_d is in all tests higher for Biax-NCF than UD-NCF despite similar materials and areal weight of the constituents in the respective directions. This potentially results from the smaller stitching pitch of the investigated Biax-NCF, but would require further studies for a conclusive claim.

The results of this study allow a better understanding of the relevant factors influencing the friction behavior of both investigated non-crimp fabrics. They can be used in forming simulation models to analyze the impact on the resulting slippage between individual plies and between plies and tools.

Acknowledgments
The authors would like to thank the Deutsche Forschungsgemeinschaft (DFG, German Research Foundation) and the French National Research Agency (ANR) for funding the collaborative project "Composite forming simulation for non-crimp fabrics based on generalized continuum approaches" (DFG: 431354059, ANR: ANR-19-CE06-0031-012), which the presented work is carried out for. This work is also part of the Heisenberg project "Digitalization of fiber-reinforced polymer processes for resource-efficient manufacturing of lightweight components", funded by the DFG (project no. 798455807141).

References

[1] W.-R. Yu, P. Harrison, A. Long, Finite element forming simulation for non-crimp fabrics using a non-orthogonal constitutive equation, Composites Part A: Applied Science and Manufacturing 36 (2005) 1079–1093. https://doi.org/10.1016/j.compositesa.2005.01.007

[2] G.D. Lawrence, S. Chen, N.A. Warrior, L.T. Harper, The influence of inter-ply friction during double-diaphragm forming of biaxial NCFs, Composites Part A: Applied Science and Manufacturing 167 (2023) 107426. https://doi.org/10.1016/j.compositesa.2023.107426

[3] U. Sachs, R. Akkerman, K. Fetfatsidis, E. Vidal-Sallé, J. Schumacher, G. Ziegmann, S. Allaoui, G. Hivet, B. Maron, K. Vanclooster, S.V. Lomov, Characterization of the dynamic friction of woven fabrics, Composites Part A: Applied Science and Manufacturing 67 (2014) 289–298. https://doi.org/10.1016/j.compositesa.2014.08.026

[4] ASTM Standard, Test Method for Static and Kinetic Coefficients of Friction of Plastic Film and Sheeting: D1894-14, ASTM International, West Conshohocken, PA, 2014

[5] N. Fulleringer, J.-F. Bloch, Forced stick-slip oscillations allow the measurement of the friction force: Application to paper materials, Tribology International 91 (2015) 94–98. https://doi.org/10.1016/j.triboint.2015.06.021

[6] S. Allaoui, G. Hivet, A. Wendling, P. Ouagne, D. Soulat, Influence of the dry woven fabrics meso-structure on fabric/fabric contact behavior, Journal of Composite Materials 46 (2012) 627–639. https://doi.org/10.1177/0021998311424627

[7] B. Cornelissen, U. Sachs, B. Rietman, R. Akkerman, Dry friction characterisation of carbon fibre tow and satin weave fabric for composite applications, Composites Part A: Applied Science and Manufacturing 56 (2014) 127–135. https://doi.org/10.1016/j.compositesa.2013.10.006

[8] S. Allaoui, C. Cellard, G. Hivet, Effect of inter-ply sliding on the quality of multilayer interlock dry fabric preforms, Composites Part A: Applied Science and Manufacturing 68 (2015) 336–345. https://doi.org/10.1016/j.compositesa.2014.10.017

[9] P. Quenzel, H. Kröger, B. Manin, K. Ngoc Vu, T.X. Duong, T. Gries, M. Itskov, R.A. Sauer, Material characterisation of biaxial glass-fibre non-crimp fabrics as a function of ply orientation, stitch pattern, stitch length and stitch tension, Journal of Composite Materials 56 (2022) 3971–3991. https://doi.org/10.1177/00219983221127005

[10] C. Poppe, D. Dörr, F. Kraus, L. Kärger, Experimental and numerical investigation of the contact behavior during FE forming simulation of continuously reinforced composites in wet compression molding, AIP Conference Proceedings 2113 (2019) 020002. https://doi.org/10.1063/1.5112507

[11] J. Hüttl, F. Albrecht, C. Poppe, F. Lorenz, B. Thoma, L. Kärger, P. Middendorf, F. Henning, Investigations on friction behaviour and forming simulation of plain woven fabrics for wet compression moulding, Proceedings of Sampe Europe, Stuttgart (2017).

[12] F. Yu, S. Chen, L.T. Harper, N.A. Warrior, Investigation into the effects of inter-ply sliding during double diaphragm forming for multi-layered biaxial non-crimp fabrics, Composites Part A: Applied Science and Manufacturing 150 (2021) 106611. https://doi.org/10.1016/j.compositesa.2021.106611

[13] F.N. Nezami, T. Gereke, C. Cherif, Analyses of interaction mechanisms during forming of multilayer carbon woven fabrics for composite applications, Composites Part A: Applied Science and Manufacturing 84 (2016) 406–416. https://doi.org/10.1016/j.compositesa.2016.02.023

[14] K.A. Fetfatsidis, D. Jauffrès, J.A. Sherwood, J. Chen, Characterization of the tool/fabric and fabric/fabric friction for woven-fabric composites during the thermostamping process, International Journal of Material Forming 6 (2013) 209–221. https://doi.org/10.1007/s12289-011-1072-5

[15] W. Najjar, C. Pupin, X. Legrand, S. Boude, D. Soulat, P. Dal Santo, Analysis of frictional behaviour of carbon dry woven reinforcement, Journal of Reinforced Plastics and Composites 33 (2014) 1037–1047. https://doi.org/10.1177/0731684414521670

[16] E.I. Avgoulas, D.M. Mulvihill, A. Endruweit, M.P.F. Sutcliffe, N.A. Warrior, D.S.A. de Focatiis, A.C. Long, Frictional behaviour of non-crimp fabrics (NCFs) in contact with a forming tool, Tribology International 121 (2018) 71–77. https://doi.org/10.1016/j.triboint.2018.01.026

[17] Y. Liu, Z. Xiang, Z. Wu, X. Hu, Experimental investigation of friction behaviors of glass-fiber woven fabric, Textile Research Journal 93 (2023) 18–32. https://doi.org/10.1177/00405175221115468

[18] L. Montero, S. Allaoui, G. Hivet, Characterisation of the mesoscopic and macroscopic friction behaviours of glass plain weave reinforcement, Composites Part A: Applied Science and Manufacturing 95 (2017) 257–266. https://doi.org/10.1016/j.compositesa.2017.01.022

[19] E. Vidal-Sallé, F. Massi, Friction Measurement on Dry Fabric for Forming Simulation of Composite Reinforcement, KEM 504-506 (2012) 319–324. https://doi.org/10.4028/www.scientific.net/KEM.504-506.319